J Neurophysiol 103: 38–46, 2010.
First published October 21, 2009; doi:10.1152/jn.00628.2009.

Enhancement of ITD Coding Within the Initial Stages of the Auditory Pathway

Michael Pecka,[1,2]* Ida Siveke,[1]* Benedikt Grothe,[1,2] and Nicholas A. Lesica[1,2]

[1]*Department of Biology II, Ludwig-Maximilians-University Munich, Martinsried; and* [2]*Bernstein Center for Computational Neuroscience, Munich, Germany*

Submitted 20 July 2009; accepted in final form 14 October 2009

Pecka M, Siveke I, Grothe B, Lesica NA. Enhancement of ITD coding within the initial stages of the auditory pathway. *J Neurophysiol* 103: 38–46, 2010. First published October 21, 2009; doi:10.1152/jn.00628.2009. Sensory systems use a variety of strategies to increase the signal-to-noise ratio in their inputs at the receptor level. However, important cues for sound localization are not present at the individual ears but are computed after inputs from the two ears converge within the brain, and we hypothesized that additional strategies to enhance the representation of these cues might be employed in the initial stages after binaural convergence. Specifically, we investigated the transformation that takes place between the first two stages of the gerbil auditory pathway that are sensitive to differences in the arrival time of a sound at the two ears (interaural time differences; ITDs): the medial superior olive (MSO), where ITD tuning originates, and the dorsal nucleus of the lateral lemniscus (DNLL), to which the MSO sends direct projections. We use a combined experimental and computational approach to demonstrate that the coding of ITDs is dramatically enhanced between these two stages, with the mutual information in the responses of single neurons increasing by a factor of 2. We also show that this enhancement is related to an increase in dynamic range for neurons with high preferred frequencies and a decrease in variability for neurons with low preferred frequencies. These results suggest that a major role of the initial stages of the ITD pathway may be to enhance the representation created at the site of coincidence detection and illustrate the potential of this pathway as a model system for the study of strategies for enhancing sensory representations in the mammalian brain.

INTRODUCTION

In the mammalian auditory pathway, the difference in the time at which a sound arrives at the two ears (interaural time differences; ITDs) provides the dominant cue for the localization of low-frequency sound sources in the horizontal plane. The primary locus of ITD tuning is the medial superior olive (MSO), a nucleus in the brain stem where the convergence of temporally precise inputs from the two ears produces variations in spike rate with changes in ITD on a microsecond time scale (Brand et al. 2002; Goldberg and Brown 1969; Pecka et al. 2008; Spitzer and Semple 1995; Yin and Chan 1990). One of the primary outputs of the MSO is a direct ascending projection to another brain stem nucleus, the dorsal nucleus of the lateral lemniscus (DNLL), but the transformation that the DNLL performs on its MSO inputs is not well understood.

Sensory transduction is inherently noisy, and sensory systems take measures to increase signal to noise ratio at or near their receptors (Faisal et al. 2008). However, ITDs are not present at the receptor level but are computed in the MSO, after inputs from the two ears have been transmitted through several synapses. The response of an MSO neuron is a degraded version of the cross-correlation of its binaural inputs (Batra and Yin 2004) and because, beyond a sharpening of tuning curves (Kuwada et al. 2006), there appears to be little qualitative difference in the ITD tuning of the MSO and DNLL, we hypothesized that the DNLL could serve to enhance the representation that is created in the MSO. To test this hypothesis, we made quantitative comparisons between both phenomenological (tuning curves) and functional (mutual information) aspects of ITD tuning in the MSO and DNLL of gerbils. Tuning curves and mutual information are complementary (the former provide a description of the representation of ITDs in the neural response, and the latter measures the efficiency of this representation), and understanding the relationship between them can provide insight into the processing strategies that underlie sensory transformations (Butts and Goldman 2006).

METHODS

Surgical and experimental procedures

Experiments were performed in accordance with the German animal welfare law (AZ 211-2531-40/01). The surgical procedures used in this study have been described in detail previously (Pecka et al. 2008; Siveke et al. 2006). Briefly, recordings were conducted in either the MSO or the DNLL of adult Mongolian gerbils (*Meriones unguiculatus*), weighing between 60 and 100 g. In all experiments, animals were initially anesthetized with an intraperitoneal injection (0.5 ml/100 g body wt) of a mixture of ketamine (20%) and xylazine (2%) diluted in 0.9% NaCl solution. Supplementary doses of 0.05–0.1 ml of the same mixture were given subcutaneously every 30 min or when needed. A previous study that explicitly compared responses in the auditory system of ketamine-anesthetized and awake gerbils (Ter-Mikaelian et al. 2007) found large differences in the cortex, but almost no differences subcortically. To gain access to the MSO, a craniotomy was performed lateral to the midline of the skull and caudal to the posterior aspect of the transverse sinus. The underlying cerebellum was partially aspirated to expose the floor of the fourth ventricle. To gain access to the DNLL, a craniotomy was performed lateral to the midline and caudal to the interaural axis. Action potentials from single neurons were recorded extracellularly using glass electrodes (impedance: 5–20 MΩ) filled with 1 M NaCl or 2% horseradish-peroxidase (HRP, Sigma-Aldrich) diluted in 10% NaCl. Action potentials were recorded, filtered, and fed into a computer via an A/D converter (RP2-1, Tucker Davis Technologies). Only recordings with high signal-to-noise ratio (>5) and stable spike waveforms were retained. Clear isolation of action potentials from single units was achieved by off-line spike cluster analysis (Brainware, Jan Schnupp). Typical recording periods lasted 10–14 h, after which animals received a

* M. Pecka and I. Siveke contributed equally to this work.

Address for reprint requests and other correspondence: N. A. Lesica, Dept. of Biology II, Ludwig-Maximilians-University Munich, Martinsried 82152, Germany (E-mail: lesica@zi.biologie.uni-muenchen.de).

lethal injection of barbital. The recording sites corresponding to 15 of the 22 MSO neurons that we analyzed were marked with HRP and histologically identified as described previously, and the other 7 neurons were judged to be in the MSO based on their physiological properties (e.g., "peak-type" ITD tuning) (Pecka et al. 2008). DNLL recordings were made in locations that were verified to be within the DNLL in previous studies, and the recorded neurons had physiological properties similar to those observed previously (Siveke et al. 2006). Some of the MSO data used in this study have been published previously (Pecka et al. 2008).

Acoustic stimuli and characterization of ITD tuning

All experiments described in this study were conducted in the same experimental setup. Acoustic stimuli were digitally generated at a sampling rate of 50 kHz and converted to analog signals (RP2-1, Tucker Davis Technologies), attenuated to desired levels (PA5, Tucker Davis Technologies) and delivered to earphones (Stereo Dynamic Earphones, MDR-EX70LP, Sony). The sound field inside the sealed system was calibrated using probe tube microphones (FG 3452, Knowles Electronics). The microphone signal was digitized (RP2-1, TDT) and transferred to the computer for off-line analysis. The difference in the sound pressure level between the two headphones was <5 dB in the range of 100–2,000 Hz and the phase difference was <0.01 cycle.

All stimuli used in this study were presented binaurally (with equal intensity at each ear) in a randomized, interleaved order and were cosine-squared gated, with a rise/fall time of 5 ms. To search for acoustic responses, 200-ms binaurally uncorrelated noise bursts (which contain no consistent ITDs) were presented. When a neuron was encountered, its characteristic phase (CP) was estimated as described previously (Pecka et al. 2008) and the best frequency (BF), the frequency at which the spike rate in response to tones at the preferred ITD was highest, was determined. Only those neurons for which the $|\,CP\,|$ <0.25 (i.e., those neurons with peak-type ITD tuning, indicating net excitatory input from the 2 ears) were included in this study. The effects of intensity on ITD tuning were characterized by repeatedly presenting 100- or 200-ms pure tone stimuli at BF at different ITDs and at a range of intensities in 5-dB steps. The range of intensities tested was different for each neuron (the lowest intensity tested for any neuron was 14 dB SPL and the highest was 89 dB SPL). The range of ITDs tested was equivalent to the duration of at least two cycles of the stimulus with eight ITDs per cycle. For the analyses in this study, the responses of all neurons to ITDs that were more than the duration of one cycle of the stimulus were combined with the responses to the corresponding ITD that was less than one cycle of the stimulus [for example, if the stimulus frequency was 1,000 Hz (and the duration of 1 cycle was 1 ms), then responses to ITDs of 0.1 and 1.1 ms were combined]. For all neurons, at least eight repetitions at each ITD (after combination) and intensity were presented. For neurons for which 200-ms stimuli were used, the last 100 ms of the responses were ignored. For population analyses, the range of intensities for each neuron was normalized relative to the lowest intensity at which the neuron exhibited significant ITD tuning as described in the preceding text. The distributions of the ITD tuning thresholds for all neurons in this study, as well as the proportion of neurons for which responses to pure tones at the intensity, frequency, and ITD that evoked the highest spike rate contained onset and sustained components, are shown in supplementary Fig. S1.[1]

Simulating MSO and DNLL responses

For each neuron, a simple model of ITD tuning was constructed as follows: first, the average spike rate at each ITD at a given intensity was modeled as a Gaussian function with peak rate, trough rate, peak ITD, and half-width matched to the experimentally measured tuning curves

$$\bar{r}_{itd} = \alpha \exp\left(\frac{-(\mathrm{ITD} - \mu)^2}{2\sigma^2}\right) + \phi \quad (1)$$

where $\bar{r}_{itd}$ is the average spike rate at a particular ITD, α = peak rate – trough rate, μ = peak ITD, σ = half-width/$2\sqrt{2\ln 2}$, and ϕ = trough rate. Then the actual spike rates at each ITD were drawn from a Laplace distribution

$$p(r_{itd}) = \frac{1}{2\omega(\bar{r}_{itd})} \exp\left(\frac{-|r_{itd} - \bar{r}_{itd}|}{\omega(\bar{r}_{itd})}\right) \quad (2)$$

where r_{itd} is the spike rate at a particular ITD and ω is the SD. The SD was modeled as a function of the average spike rate based on the experimentally measured variability with

$$\omega(\bar{r}_{itd}) = [\beta \bar{r}_{itd}\, e^{-\bar{r}_{itd}/\nu}]^{1/2} \quad (3)$$

where β and ν were fit based on the relationship between the Fano factor and the average spike rate measured at each ITD and each intensity for each neuron. Negative values of r_{itd} were mapped to zero. Several other distributions for the variability in spike rates about the mean were tested, but the Laplace distribution yielded the best fits (see Supplementary Fig. S2).

Calculation of mutual information

The mutual information between the stimulus ITD and the spike rate in simulated and experimental responses at a given intensity was calculated as (Borst and Theunissen 1999)

$$I(r, \mathrm{ITD}) = \sum_i \sum_j p(\mathrm{ITD}_j) p(r_i \mid \mathrm{ITD}_j) \log_2[p(r_i \mid \mathrm{ITD}_j)/p(r_i)] \quad (4)$$

where $p(\mathrm{ITD}_j)$ is the probability that the stimulus ITD had a particular value, ITD_j (in this study, all ITDs were presented with equal probability), $p(r_i)$ is the probability that the spike rate had a particular value r_i at any ITD (in this study, possible values for r_i corresponded to integer spike counts between 0 and 100 for a 100-ms stimulus), and $p(r_i \mid \mathrm{ITD}_j)$ is the probability that the spike rate had value r_i when the ITD had value ITD_j. For calculating the information in experimental responses, different numbers of repeated stimulus presentations at each ITD were used to verify the stability of the information measures, as described in Supplementary Fig. S2. For calculating the information in simulated responses, 1,000 repeated stimulus presentations at 64 ITDs within the physiological range were used.

RESULTS

To determine how the neural representation of ITDs is transformed within the initial stages of the auditory pathway, we studied the ITD tuning of neurons in the MSO (n = 22) and DNLL (n = 25) of anesthetized gerbils. Only DNLL neurons that exhibited peak-type ITD tuning (characteristic phase: <0.25), suggesting that they received net excitation from both ears and thus that their dominant input was the MSO, were included. To characterize ITD tuning, pure tone stimuli at each neuron's BF were presented through headphones at a range of ITDs and overall intensities. Across the populations that were analyzed, the BFs in the MSO and DNLL were not significantly different (MSO: 250–1,250 Hz; DNLL: 400–1,200 Hz; Wilcoxon rank sum test, P = 0.36) nor were the lowest intensities at which significant ITD tuning (based on the Raleigh test) was observed (MSO: 15–59 dB SPL; DNLL: 14–59 dB SPL; Wilcoxon rank sum test, P = 0.07). The distributions of the

[1] The online version of this article contains Supplemental material.

BFs and ITD tuning thresholds, as well as the response types (onset, sustained, etc.) for all neurons in this study are shown in Supplementary Fig. S1.

ITD tuning curves in the MSO and DNLL

To provide a phenomenological characterization of MSO and DNLL responses, we measured the tuning curves that related the spike rate to ITD at different intensities. Example tuning curves for two MSO and two DNLL neurons are shown in Fig. 1, *A* and *B*. Each line represents the average spike rate across repeated stimulus presentations at a particular intensity and the error bars denote 1 SD from the average. The physiological range of ITDs (the range of ITDs that can actually be produced by a single sound source) is denoted by the black vertical bars (approximately ± 135 μs for gerbils) (Maki and Furukawa 2005).

As a preliminary characterization of ITD tuning, we extracted four parameters from each tuning curve: the *peak* (the highest average spike rate), *trough* (the lowest average spike rate), *peak ITD* (the ITD that evoked the highest average spike rate), and *half-width* {the range of ITDs for which the average spike rate was above [trough rate + (peak rate – trough rate)/2]}. To characterize the effects of intensity on these parameters across the populations of neurons from which we recorded, we calculated the median tuning curve parameter values at different intensities, starting 5 dB above the ITD tuning threshold for each neuron and increasing to 20–30 dB above this threshold (a range across which the spike rates of inputs to the MSO are likely to increase linearly with increasing intensity) (Joris et al. 1994; Rhode and Smith 1986; Winter and Palmer 1990).

Figure 2 shows the effects of intensity on each tuning curve parameter in the MSO and DNLL. Each gray line shows the parameter value for an individual neuron and the black line shows the population median. The peak started at similar values in the MSO and DNLL and increased significantly with increasing intensity in both nuclei (Wilcoxon rank sum test, MSO: $P < 0.001$, DNLL: $P < 0.001$), such that the peak in the MSO and DNLL was not significantly different at either low [5 dB normalized intensity (NI)] or high (30 dB NI) intensity (Wilcoxon rank sum test, 5 dB: $P = 0.32$, 30 dB: $P = 0.75$). The trough also started at similar values in the MSO and DNLL but increased significantly with increasing intensity in the MSO (Wilcoxon rank sum test, $P < 0.001$) and remained relatively constant with increasing intensity in the DNLL (Wilcoxon rank sum test, $P = 0.15$). As a result, the trough rate in the MSO and DNLL was not significantly different at low intensity (Wilcoxon rank sum test, $P = 0.23$), but the trough rate in the MSO was significantly larger than that in the DNLL at high intensity (Wilcoxon rank sum test, $P < 0.001$). In the MSO, both the peak ITD and half-width were relatively invariant to changes in intensity. In the DNLL, the peak ITD was also invariant to changes in intensity, but the half-width decreased significantly with increasing intensity (Wilcoxon rank

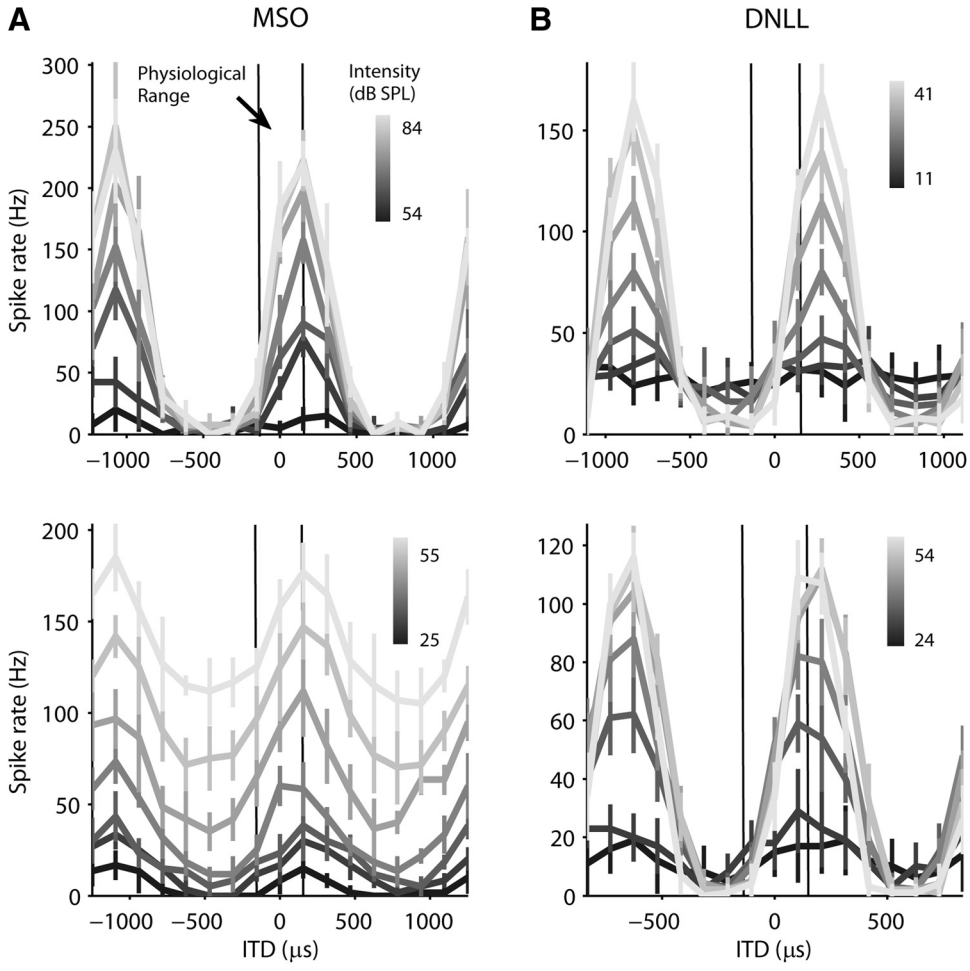

FIG. 1. The interaural time difference (ITD) tuning of single neurons in the medial superior olive (MSO) and dorsal nucleus of the lateral lemniscus (DNLL). *A*: the tuning curves relating spike rate to ITD at several intensities for 2 MSO neurons. The lines (colored according to intensity) show the spike rate averaged across repeated stimulus presentations, and the error bars denote 1 SD from the average. The BFs for the neurons were 800 and 817 Hz. *B*: the tuning curves relating spike rate to ITD at several intensities for 2 DNLL neurons, presented as in *A*. The best frequencies (BFs) for the neurons were 900 and 1,200 Hz.

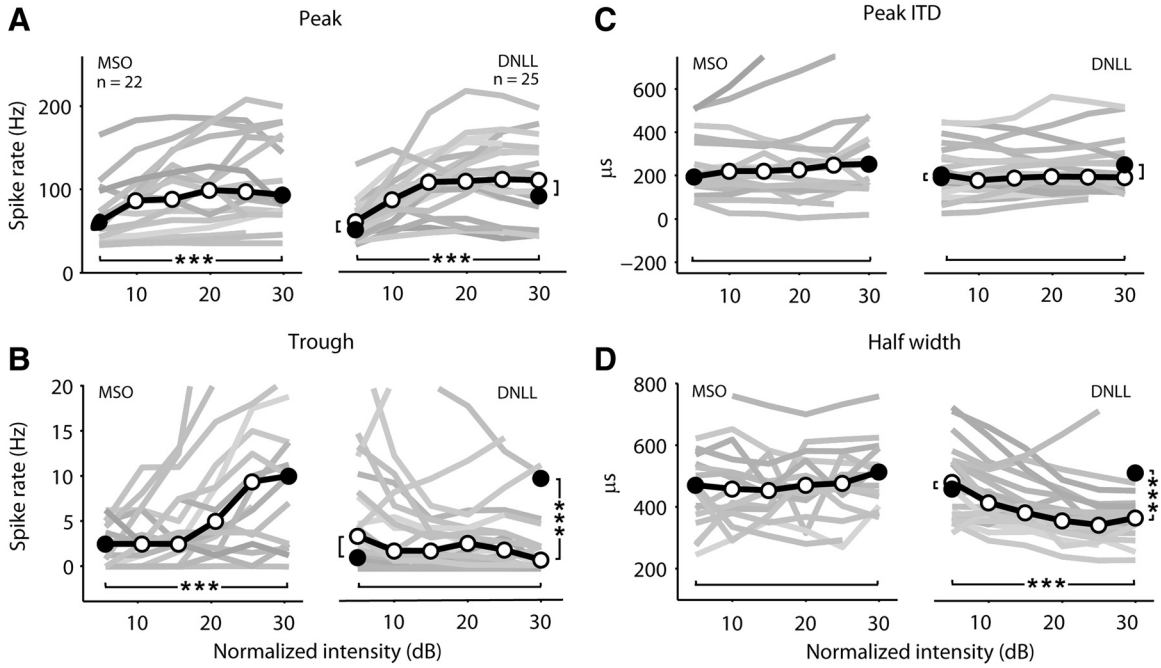

FIG. 2. The effects of intensity on the parameters of ITD tuning curves in the MSO and DNLL. *A, left* and *right*: the peak of the ITD tuning curves for MSO and DNLL neurons, respectively, (gray lines) along with the population medians (black line) as a function of normalized intensity (NI; intensity relative to the lowest at which each neuron exhibited significant ITD tuning according to the Rayleigh test; see METHODS). The median values of the parameters for MSO neurons at 5 and 30 dB NI are shown as filled circles in both the *left* and *right panels.* The *P* values for Wilcoxon rank sum tests indicating the probability that values from the same nucleus at different intensities or different nuclei at the same intensity came from distributions with the same median are shown (*$P < 0.05$, **$P < 0.01$, ***$P < 0.001$). *B–D*: the trough, peak ITD, and half-width of ITD tuning curves for neurons in the MSO and DNLL, presented as in *A*.

sum test, $P < 0.001$), such that the half-width in the MSO and DNLL was not significantly different at low intensity (Wilcoxon rank sum test, $P = 0.2$), but the half-width in the MSO was significantly larger than that in the DNLL at high intensity (Wilcoxon rank sum test, $P < 0.001$).

Dynamic range of ITD tuning in the MSO and DNLL

As a first step toward understanding the relationship between the phenomenological and functional aspects of ITD tuning in the MSO and DNLL, we measured the dynamic range (peak – trough) of the ITD tuning curves for each neuron at each intensity. Changes in dynamic range can have important functional implications: an increase in dynamic range implies an increase, on average, in the difference in the responses to similar ITDs, thus potentially making those ITDs easier to distinguish.

Figure 3*A* shows the effects of intensity on dynamic range in the MSO and the DNLL. In both nuclei, the population median dynamic range started at ~40 Hz and increased significantly with increasing intensity (Wilcoxon rank sum test, MSO: $P = 0.005$, DNLL: $P < 0.001$), such that the population median dynamic range in the MSO and DNLL was not significantly different at either low or high intensity (Wilcoxon rank sum test, 5 dB: $P = 0.32$, 30 dB: $P = 0.33$). The change in dynamic range with increasing intensity in both nuclei was due primarily to changes in the tuning curve peak and was influenced little by changes in the tuning curve trough (partial least-squares linear regression, MSO: percentage variance explained by peak = 92%, percentage variance explained by trough = 8%; DNLL: percentage variance explained by peak = 98%, percentage variance explained by trough = 2%).

The preceding results suggest that across the entire population, the dynamic range of ITD tuning curves in the MSO and DNLL are similar. However, a closer look at the relationship between dynamic range and BF in the MSO and DNLL revealed an important difference. We measured the correlation coefficient between dynamic range and BF at 20 dB NI (to minimize the effects of extreme values on measurement of correlation coefficients, values >3 SD above or below the mean were not included). As shown in Fig. 3*B,* dynamic range decreased with increasing BF in the MSO ($r = -0.53$, $P = 0.02$) but was independent of BF in the DNLL ($r = 0.37$, $P = 0.07$). As a result, while the dynamic range in the MSO and DNLL was not significantly different for neurons with low BFs (≤800 Hz, the median BF in the MSO; Wilcoxon rank sum test, $P = 0.71$, MSO: median value = 87.1, $n = 12$; DNLL: median value = 99.9, $n = 10$), the dynamic range in the DNLL was significantly larger than that in the MSO for neurons with high BFs (>800 Hz; Wilcoxon rank sum test, $P = 0.006$, MSO: median value = 29.7, $n = 10$; DNLL: median value = 107.9, $n = 15$).

Variability of ITD tuning in the MSO and DNLL

Dynamic range is not the only property of ITD tuning curves with an important functional role. In fact, the functional consequences of changes in dynamic range can only be accurately judged relative to the corresponding changes in response variability: simply doubling the spike rate for a neuron would not make it any easier to distinguish between similar ITDs as the resulting increases in dynamic range and variability would offset each other. To characterize the variability of ITD tuning in the MSO and DNLL, we computed the Fano factor, the ratio

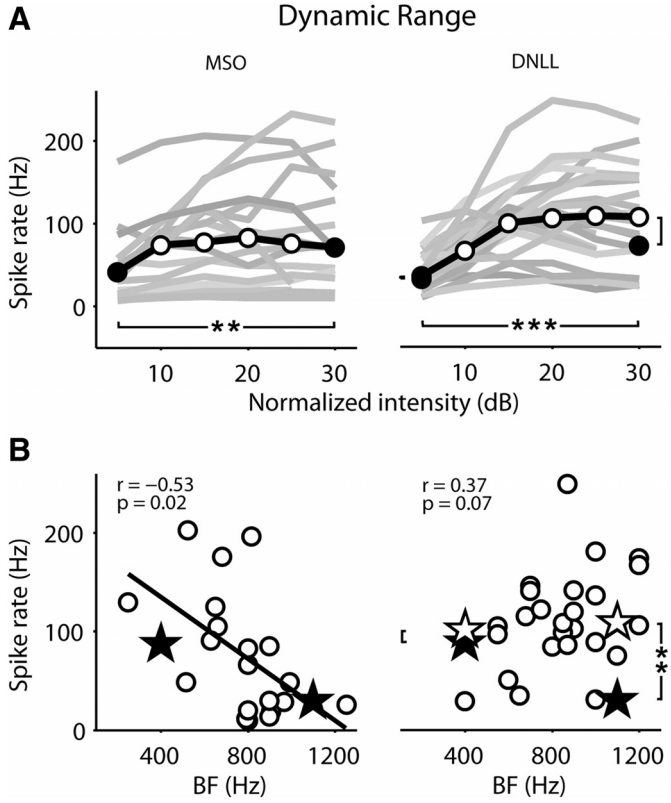

FIG. 3. The effects of intensity and BF on the dynamic range of ITD tuning in the MSO and DNLL. *A, left* and *right*: the dynamic range (peak – trough) of the ITD tuning curves for MSO and DNLL neurons, respectively, as a function of normalized intensity, presented as in Fig. 2. *B, left* and *right*: scatter plots of the dynamic range at 20 dB NI vs. BF for MSO and DNLL neurons, respectively. The median values for MSO neurons with low BFs (≤800 Hz) and high BFs (>800 Hz) are shown in both panels (★) and the median values for DNLL neurons with low and high BFs are shown *right* (☆). The correlation coefficients and corresponding *P* values are shown, along with the best linear fit for significantly correlated data (MSO only).

of the variance of the spike rate to its mean, at the peak of the ITD tuning curves (FF_{peak}) for each neuron at each intensity. As shown in Fig. 4*A*, the population median value of FF_{peak} was ~0.5 in both the MSO and DNLL at low intensity, but although FF_{peak} remained relatively constant with increasing intensity in the MSO (Wilcoxon rank sum test, $P = 0.99$), it decreased significantly with increasing intensity in the DNLL (Wilcoxon rank sum test, $P < 0.001$). As a result, FF_{peak} was not significantly different in the MSO and DNLL at low intensity (Wilcoxon rank sum test, $P = 0.37$), but FF_{peak} was significantly lower in the DNLL than in the MSO at high intensity (Wilcoxon rank sum test, $P < 0.001$).

We also examined the relationship between variability and BF. As shown in Fig. 4*B*, FF_{peak} decreased with increasing BF in the MSO ($r = -0.54$, $P = 0.01$) but was independent of BF in the DNLL ($r = -0.06$, $P = 0.80$). As a result, FF_{peak} in the MSO was significantly larger than that in DNLL for neurons

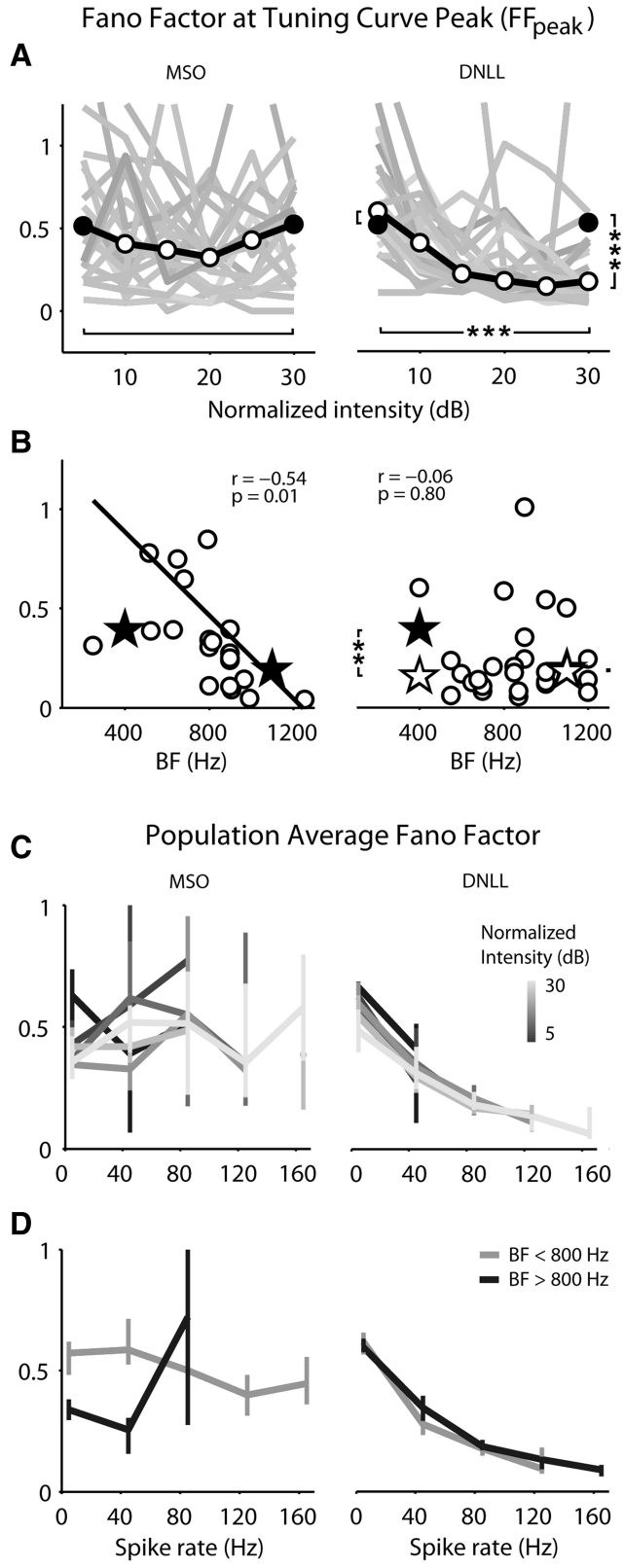

FIG. 4. The effects of intensity and BF on the variability of ITD tuning in the MSO and DNLL. *A, left* and *right*: the Fano factor, the ratio of the variance of the spike rate to its mean, at the peak of the ITD tuning curves (FF_{peak}) for MSO and DNLL neurons, respectively, as a function of normalized intensity, presented as in Fig. 2. *B, left* and *right*: scatter plots of FF_{peak} at 20 dB NI vs. BF for MSO and DNLL neurons, respectively, presented as in Fig. 3*B*. *C, left* and *right*: the population median Fano factor including responses to all ITDs as a function of average spike rate for each intensity. The error bars denote 95% confidence intervals for the median values. *D, left* and *right*: the population median Fano factor including responses to all ITDs as a function of average spike rate for neurons with low BFs (≤800 Hz) and high BFs (>800 Hz), respectively. The error bars denote 95% confidence intervals for the median values.

with low BFs (≤800 Hz; Wilcoxon rank sum test, $P = 0.007$, MSO: median value = 0.39, $n = 12$; DNLL: median value = 0.15, $n = 10$) but not for neurons with high BFs (>800 Hz; Wilcoxon rank sum test, $P = 0.63$, MSO: median value = 0.19, $n = 10$; DNLL: median value = 0.17, $n = 15$).

The preceding results suggest that variability changes with BF across the population in the MSO and with intensity for single neurons in the DNLL. However, because the Fano factor is a function of the average spike rate, and the average spike rates (as evidenced by the dynamic range) can change with BF and intensity, the preceding results do not distinguish between changes in variability that are dependent on intensity or BF per se, and changes in variability that are dependent only on changes in the average spike rate. To distinguish between these two possibilities, we measured the median Fano factor across the population as a function of average spike rate for different intensities and BFs (including responses not only from the peak of the ITD tuning curve, but for all ITDs). In Fig. 4*C,* each line shows the median Fano factor across the population as a function of average spike rate for a given intensity (error bars indicate 95% confidence intervals, estimated using the binomial distribution) (Conover 1980). In both nuclei, the relationship between Fano factor and average spike rate was similar across intensities, suggesting that the observed changes in variability with intensity in the DNLL are not in fact intensity dependent but are a consequence of the corresponding changes in dynamic range. In Fig. 4*D,* the two lines show the median Fano factor across the population as a function of average spike rate for neurons with low BFs (≤800 Hz; MSO: $n = 12$, DNLL: $n = 10$) and high BFs (>800 Hz; MSO: $n = 10$, DNLL: $n = 15$). In the MSO, at low average spike rates, the Fano factor for neurons with high BFs was lower than that for neurons with low BFs, while in the DNLL, the relationship between Fano factor and average spike rate was similar for neurons with high and low BFs. This result suggests that the observed changes in variability in the MSO are indeed dependent on changes in BF and are not simply a consequence of corresponding changes in dynamic range.

Mutual information between spike rate and ITD in the MSO and DNLL

The effects of BF and intensity on the dynamic range and variability in the MSO and DNLL suggest potential functional differences in the ITD tuning in these two nuclei. To provide a functional characterization of ITD tuning in the MSO and DNLL, we calculated the mutual information between ITD and spike rate for each neuron at each intensity (as spike timing has been shown to contain little information about ITD) (Chase and Young 2006). Because calculating mutual information required sampling the response in the physiological range with a higher resolution than we used in our experiments, we developed a simple model for MSO and DNLL responses. The basis for the model is provided by the ITD tuning curves, which characterize both the mean and variability in the spike rate. To define the model, we fit the experimental responses for each neuron with parametric functions: the average spike rate at each ITD was modeled as a Gaussian function, and the distribution of spike rates about the average at each ITD was modeled as a Laplace function with SD that varied as function of the average rate (see METHODS for details and Supplementary Fig. S2 for examples and model validation).

Using this model, we simulated the responses of each neuron in the MSO and DNLL to 1,000 repeated presentations of 64 ITDs that were evenly spaced within the physiological range and measured the information in the responses. As shown in Fig. 5*A,* the population median information in the MSO and DNLL was not significantly different at low intensity (Wilcoxon rank sum test, $P = 0.66$) with a value of ~1.2 bits. In the MSO, the information remained relatively constant with increasing intensity (Wilcoxon rank sum test, $P = 0.36$), but in the DNLL, the information increased significantly with increasing intensity to ~2.4 bits (Wilcoxon rank sum test, $P < 0.001$). Thus at higher intensities, the median information in DNLL responses was significantly higher than that in MSO responses (Wilcoxon rank sum test, $P = 0.009$).

We also examined the relationship between information and BF in the MSO and DNLL. As shown in Fig. 4*B,* information was independent of BF in both the MSO ($r = 0.11$, $P = 0.65$) and DNLL ($r = 0.18$, $P = 0.39$), and the information in the DNLL was higher in that in the MSO for neurons with both low BFs (≤800 Hz; Wilcoxon rank sum test, $P = 0.03$, MSO: median value = 1.32, $n = 12$; DNLL: median value = 1.98, $n = 10$) and high BFs (>800 Hz; Wilcoxon rank sum test, $P =$

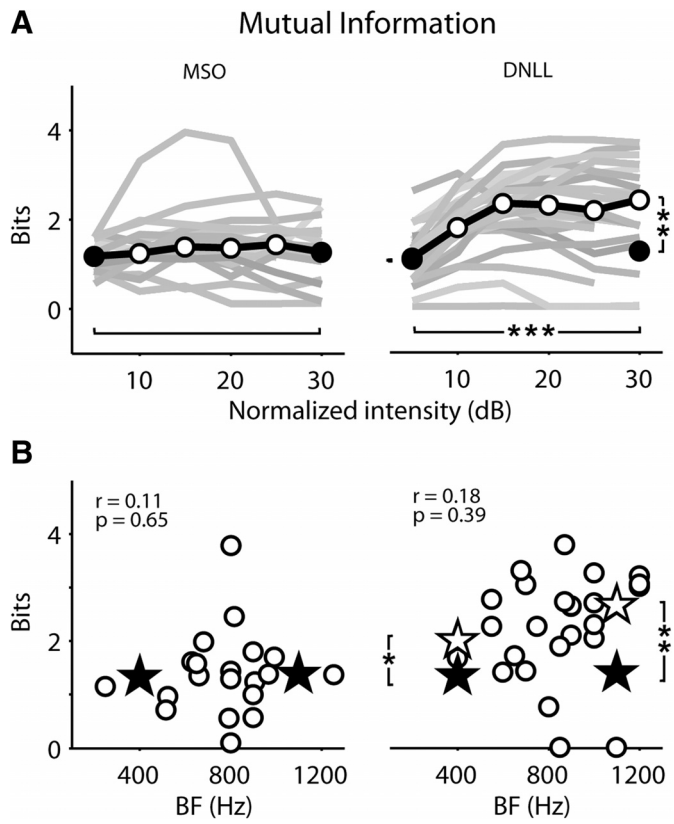

FIG. 5. The effects of intensity and BF on the mutual information between spike rate and ITD in the MSO and DNLL. *A, left* and *right*: the mutual information in the responses of MSO and DNLL neurons, respectively, as a function of normalized intensity, presented as in Fig. 2. The mutual information was computed from the simulated responses of each neuron to ITDs within the physiological range, as described in supplementary Fig. 2. *B, left* and *right*: scatter plots of the information in the responses of MSO and DNLL neurons at 20 dB NI vs. BF, presented as in Fig. 3*B.*

0.01, MSO: median value = 1.38, $n = 10$; DNLL: median value = 2.62, $n = 15$).

DISCUSSION

Our experimental and simulated results indicate that the neural representation of ITDs is enhanced from the MSO to the DNLL. In the MSO, changes in dynamic range and variability offset each other such that the information in MSO responses was relatively constant across intensities and BFs. In the DNLL, intensity dependent changes in dynamic range and variability complement each other such that at high intensity, the dynamic range in the DNLL was higher than that in the MSO for neurons with high BFs and the variability in the DNLL was lower than that in the MSO for neurons with low BFs. As a result, the information in DNLL responses at high intensity was nearly twice that of MSO responses for neurons with both low and high BFs. Given the lack of strong qualitative differences in ITD tuning between the MSO and DNLL, and the magnitude of the enhancement that we observed, it is likely that increasing signal to noise ratio is one of the major roles of the initial stages of the mammalian ITD pathway.

Intensity- and BF-dependent changes in ITD tuning in the MSO and DNLL

Although we observed increases in the dynamic range of ITD tuning with increasing intensity in both the MSO and DNLL, it was only in the DNLL that this increase was paired with a corresponding decrease in variability. Thus while the information in MSO responses remained constant with increasing intensity, the information in DNLL responses increased. Our results suggest that the increase in information in the DNLL at high intensities was due to mechanisms that decrease the variability of MSO inputs without sacrificing dynamic range for neurons with low BFs and increase the dynamic range of MSO inputs without increasing variability for neurons with high BFs. Whether these effects originate from different mechanisms or are BF dependent manifestations of the same mechanism is a topic for future research.

The decreases in both dynamic range and variability in the MSO that we observed with increasing BF are consistent with idea that the generation of ITD tuning in the MSO is reliant on phase-locked, cycle-by-cycle inhibition that interacts with binaural excitation (Pecka et al. 2008). For neurons with low BFs, the time constant of the inhibitory inputs, ~1–2 ms (Magnusson et al. 2005), may be fast enough to prevent spilling over into the next cycle, but for neurons with high BFs, while the inhibition is still modulated on a cycle-by-cycle basis, the build-up of inhibition across successive cycles may create a state of tonic inhibition and thus reduce spike rates and variability. Our results suggest that the processing of MSO inputs in the DNLL is matched to the temporal constraints of the ITD generation mechanism, decreasing the variability of inputs with low BFs that already have a large dynamic range and increasing the dynamic range of inputs with high BFs that already have a low variability.

Transformations along the mammalian auditory pathway

Previous studies have noted several transformations in the neural representation of ITDs that take place along the ascending mammalian auditory pathway: increasing sensitivity to stimulus context, increasing preference for ITDs that correspond to sounds on the contralateral side and sharpening of ITD tuning curves (Fitzpatrick et al. 1997, 2002; Kuwada et al. 2006; Spitzer and Semple 1998). It has also been suggested that the latter transformation results in an increase in the acuity of the ITD population code (Fitzpatrick et al. 1997). This suggestion was based on the assumption that neurons in the mammalian auditory pathway employ a labeled-line code similar to the one used by birds (for review, see Konishi 2003).Using simulations based on experimental data, Fitzpatrick et al. showed that if the neurons are organized into a "space map" according to their peak ITDs, then the sharpening of tuning curves at successive auditory stages can decrease the minimum detectable change in ITD based on population responses. However, efforts to find a space map in the ascending mammalian ITD pathway have been unsuccessful (Middlebrooks et al. 2002), and recent studies have shown that the ITDs that correspond to the tuning curve peaks for most neurons with low preferred frequencies in the mammalian brain stem and midbrain are not distributed across the physiological range but instead near the edge of the physiological range, while the ITDs where the slope of the tuning curve is maximal cluster near zero (Brand et al. 2002; Hancock and Delgutte 2004; McAlpine et al. 2001; Pecka et al. 2008; Siveke et al. 2006). These findings suggest that mammals do not use a labeled line code but instead utilize a population rate code with each neuron responding to the entire physiological range of ITDs with variations in spike rate (Brand et al. 2002; Harper and McAlpine 2004; McAlpine and Grothe 2003; McAlpine et al. 2001). Our analysis, which does not assume that the mammalian auditory system contains a space map but simply measures the information available in the responses of individual neurons within the MSO and DNLL, suggests that the differences in the dynamic range and variability of neurons in these two nuclei have an important functional role. Thus the transformation that takes place between the MSO to the DNLL does not appear to change the nature of the neural representation of ITDs but rather to increase the efficiency of the representation that is created at the initial site of binaural convergence.

Comparison with previous studies in mammals and birds

No previous studies have compared the efficiency of ITD tuning in the responses of single neurons along the mammalian ITD pathway. There has also been little study of ITD tuning at different intensities in the MSO or DNLL, but the effects of intensity on ITD tuning curves that have been reported are at least qualitatively similar to those that we observed in this study (Goldberg and Brown 1969).

The avian auditory system also computes ITDs within the brain after the convergence of inputs from the two ears. Despite the differences in the circuitry used to create ITD tuning in the mammalian and avian auditory systems (Grothe 2003; McAlpine and Grothe 2003), the reduction of noise in the initial stages of the ITD pathway appears to be a common strategy in both systems. As with the MSO, the ability of neurons in nucleus laminaris (NL; the initial site of binaural convergence in birds) to encode ITDs, as measured by, for example, dynamic range, is relatively invariant to changes in intensity (Pena et al. 1996) [however, in the bird, this invari-

ance appears to be dependent on inhibitory input from the superior olivary nucleus (Nishino et al. 2008), a structure with no clear equivalent in mammals]. In comparison to NL, the ITD tuning curves of neurons in the next two stages of the avian ITD pathway, the dorsal lateral lemniscus nucleus (LLDa) and the core of the inferior colliculus (ICcc), have less variability and larger dynamic range than those in NL, and responses in the LLDa and ICcc contain more Fisher information (Christianson and Pena 2006; Fischer and Konishi 2008). It has been hypothesized that the enhanced coding of ITDs observed in LLDa and ICcc is due to the convergence of NL inputs (indeed convergence is a requirement, given that the information in the responses of single neurons in LLDa and ICcc is larger than that in the responses of single neurons in NL). It is likely that convergence of MSO inputs also plays a role in the enhanced coding of ITDs that we observe in the DNLL, but the complex circuitry of the mammalian auditory brain stem also presents other possibilities (see following text).

Possible roles for the DNLL in the processing of ITDs

The DNLL has already been shown to play an important role in the processing of interaural level differences (Faingold et al. 1993; Li and Kelly 1992) and echoes (Burger and Pollak 2001; Pecka et al. 2007; Pollak 1997). Our results suggest that another important role of the DNLL may be to enhance the neural representation of ITDs that is created in the MSO by increasing its dynamic range and decreasing its variability. While part of this enhancement may arise from the convergence of MSO inputs in the DNLL (as described in the preceding text, convergence has been suggested to underlie the enhancement observed in early stages of the ITD pathway in birds) (Christianson and Pena 2006; Fischer and Konishi 2008), it is also possible that this enhancement may be furthered by the reciprocal connections of the DNLL with its contralateral counterpart. The two DNLLs are connected via inhibitory projections that cross the commissure of Probst and have opposing ITD tuning (i.e., the ITDs that correspond to the peak rate in the responses of one DNLL correspond to the trough rate in the other DNLL, and vice versa). Thus the inhibitory inputs to one DNLL from its contralateral counterpart will be weak at ITDs that correspond to the peak rate of its MSO inputs but strong at ITDs that correspond to the trough rate of its MSO inputs, and, thus could suppress the MSO inputs at these ITDs. This scheme could, for example, allow the peak rate in the DNLL output to increase with increasing intensity without a corresponding increase in the trough rate, resulting in an increase in dynamic range. It is also possible that inhibitory projections from the DNLL could serve a similar function at higher levels. For example, the DNLL sends strong inhibitory projections to the contralateral IC (Shneiderman and Oliver 1989), and these inputs could serve to suppress IC responses to ITDs that correspond to the trough rate of MSO inputs with opposing ITD tuning.

It should also be noted that our results are restricted to DNLL neurons with peak-type ITD tuning (i.e., those that likely receive input from the MSO). The DNLL also contains many neurons with "trough-type" ITD tuning, which likely receive inputs from the lateral superior olive (LSO). The mechanism that is responsible for ITD tuning in the LSO is reliant on the same phase-locked, cycle-by-cycle inhibition that is important for ITD tuning in the MSO. Thus some of the same intensity- and BF-dependent changes in dynamic range and variability that we observed in the MSO may also be apparent in the LSO and, consequently, in the inputs to trough-type neurons in the DNLL. Whether these DNLL neurons also serve to increase the signal-to-noise ratio in their inputs, and, indeed, how these neurons interact with peak-type neurons to form the overall representation of ITDs, are questions for future research.

The changes in dynamic range and variability that we observe from the MSO to the DNLL may be important not only for improving the coding of ITDs for a single sound source, as suggested by our results, but also for facilitating the localization of sounds in the presence of background noise. Using a combination of simulated and experimental results, Siveke et al. (2007) showed that the addition of broadband noise to a pure tone stimulus degraded ITD tuning in both the MSO and DNLL. In the MSO, the addition of noise caused in a large increase in the trough rate of the ITD tuning curve, but only a small increase in the peak rate, resulting in a large decrease in dynamic range. In the DNLL, this decrease in dynamic range was reduced, as the addition of noise caused only a small change in the trough rate. Thus differences in the dynamic range of neurons in the MSO and DNLL appear to effect the coding of ITDs for single sound sources and in the presence of background noise.

ACKNOWLEDGMENTS

We thank A. Klug, C. Leibold, and L. Wiegrebe for helpful discussions.

GRANTS

This work was supported by the Bernstein Center for Computational Neuroscience and Deutsche Forschungsgemeinschaft Grants GR1205/12-1 and LE2522/1-1). I. Siveke was supported by the Deutsche Studienstiftung.

REFERENCES

Batra R, Yin TCT. Cross correlation by neurons of the medial superior olive: a reexamination. *J Assoc Res Otolaryngol* 5: 238–252, 2004.

Borst A, Theunissen FE. Information theory and neural coding. *Nat Neurosci* 2: 947–957, 1999.

Brand A, Behrend O, Marquardt T, McAlpine D, Grothe B. Precise inhibition is essential for microsecond interaural time difference coding. *Nature* 417: 543–547, 2002.

Burger RM, Pollak GD. Reversible inactivation of the dorsal nucleus of the lateral lemniscus reveals its role in the processing of multiple sound sources in the inferior colliculus of bats. *J Neurosci* 21: 4830–4843, 2001.

Butts DA, Goldman MS. Tuning curves, neuronal variability, and sensory coding. *PLoS Biol* 4: e92, 2006.

Chase SM, Young ED. Spike-timing codes enhance the representation of multiple simultaneous sound-localization cues in the inferior colliculus. *J Neurosci* 26: 3889–3898, 2006.

Christianson GB, Pena JL. Noise reduction of coincidence detector output by the inferior colliculus of the barn owl. *J Neurosci* 26: 5948–5954, 2006.

Conover, WJ. *Practical Nonparametric Statistics.* New York: Wiley, 1980.

Faingold CL, Anderson CA, Randall ME. Stimulation or blockade of the dorsal nucleus of the lateral lemniscus alters binaural and tonic inhibition in contralateral inferior colliculus neurons. *Hear Res* 69: 98–106, 1993.

Faisal AA, Selen LP, Wolpert DM. Noise in the nervous system. *Nat Rev Neurosci* 9: 292–303, 2008.

Fischer BJ, Konishi M. Variability reduction in interaural time difference tuning in the barn owl. *J Neurophysiol* 2008.

Fitzpatrick DC, Batra R, Stanford TR, Kuwada S. A neuronal population code for sound localization. *Nature* 388: 871–874, 1997.

Fitzpatrick DC, Kuwada S, Batra R. Transformations in processing interaural time differences between the superior olivary complex and inferior colliculus: beyond the Jeffress model. *Hear Res* 168: 79–89, 2002.

Goldberg JM, Brown PB. Response of binaural neurons of dog superior olivary complex to dichotic tonal stimuli: some physiological mechanisms of sound localization. *J Neurophysiol* 32: 613–636, 1969.

Grothe B. New roles for synaptic inhibition in sound localization. *Nat Rev Neurosci* 4: 540–550, 2003.

Hancock KE, Delgutte B. A physiologically based model of interaural time difference discrimination. *J Neurosci* 24: 7110–7117, 2004.

Harper NS, McAlpine D. Optimal neural population coding of an auditory spatial cue. *Nature* 430: 682–686, 2004.

Joris PX, Carney LH, Smith PH, Yin TC. Enhancement of neural synchronization in the anteroventral cochlear nucleus. I. Responses to tones at the characteristic frequency. *J Neurophysiol* 71: 1022–1036, 1994.

Konishi M. Coding of auditory space. *Annu Rev Neurosci* 26: 31–55, 2003.

Kuwada S, Fitzpatrick DC, Batra R, Ostapoff EM. Sensitivity to interaural time differences in the dorsal nucleus of the lateral lemniscus of the unanesthetized rabbit: comparison with other structures. *J Neurophysiol* 95: 1309–1322, 2006.

Kuwada S, Stanford TR, Batra R. Interaural phase-sensitive units in the inferior colliculus of the unanesthetized rabbit: effects of changing frequency. *J Neurophysiol* 57: 1338–1360, 1987.

Li L, Kelly JB. Inhibitory influence of the dorsal nucleus of the lateral lemniscus on binaural responses in the rat's inferior colliculus. *J Neurosci* 12: 4530–4539, 1992.

Magnusson A. K, Kapfer C, Grothe B, Koch U. Maturation of glycinergic inhibition in the gerbil medial superior olive after hearing onset. *J Physiol* 568: 497–512, 2005.

Maki K, Furukawa S. Acoustical cues for sound localization by the Mongolian gerbil, *Meriones unguiculatus. J Acoust Soc Am* 118: 872–886, 2005.

Mardia KV. *Statistics of Directional Data.* London: Academic, 1972.

McAlpine D, Grothe B. Sound localization and delay lines–do mammals fit the model?. *Trends Neurosci* 26: 347–350, 2003.

McAlpine D, Jiang D, Palmer AR. A neural code for low-frequency sound localization in mammals. *Nat Neurosci* 4: 396–401, 2001.

Middlebrooks JC, Xu L, Furukawa S, Macpherson EA. Cortical neurons that localize sounds. *Neuroscientist* 8: 73–83, 2002.

Nishino E, Yamada R, Kuba H, Hioki H, Furuta T, Kaneko T, Ohmori H. Sound-intensity-dependent compensation for the small interaural time difference cue for sound source localization. *J Neurosci* 28: 7153–7164, 2008.

Pecka M, Brand A, Behrend O, Grothe B. Interaural time difference processing in the mammalian medial superior olive: the role of glycinergic inhibition. *J Neurosci* 28: 6914–6925, 2008.

Pecka M, Zahn TP, Saunier-Rebori B, Siveke I, Felmy F, Wiegrebe L, Klug A, Pollak GD, Grothe B. Inhibiting the inhibition: a neuronal network for sound localization in reverberant environments. *J Neurosci* 27: 1782–1790, 2007.

Pena JL, Viete S, Albeck Y, Konishi M. Tolerance to sound intensity of binaural coincidence detection in the nucleus laminaris of the owl. *J Neurosci* 16: 7046–7054, 1996.

Pollak GD. Roles of GABAergic inhibition for the binaural processing of multiple sound sources in the inferior colliculus. *Ann Otol Rhinol Laryngol Suppl* 168: 44–54, 1997.

Rhode WS, Smith PH. Encoding timing and intensity in the ventral cochlear nucleus of the cat. *J Neurophysiol* 56: 261–286, 1986.

Shneiderman A, Oliver DL. EM autoradiographic study of the projections from the dorsal nucleus of the lateral lemniscus: a possible source of inhibitory inputs to the inferior colliculus. *J Comp Neurol* 286: 28–47, 1989.

Siveke I, Leibold C, Grothe B. Spectral composition of concurrent noise affects neuronal sensitivity to interaural time differences of tones in the dorsal nucleus of the lateral lemniscus. *J Neurophysiol* 98: 2705–2715, 2007.

Siveke I, Pecka M, Seidl AH, Baudoux S, Grothe B. Binaural response properties of low-frequency neurons in the gerbil dorsal nucleus of the lateral lemniscus. *J Neurophysiol* 96: 1425–1440, 2006.

Spitzer MW, Semple MN. Neurons sensitive to interaural phase disparity in gerbil superior olive: diverse monaural and temporal response properties. *J Neurophysiol* 73: 1668–1690, 1995.

Spitzer MW, Semple MN. Transformation of binaural response properties in the ascending auditory pathway: influence of time-varying interaural phase disparity. *J Neurophysiol* 80: 3062–3076, 1998.

Ter-Mikaelian M, Sanes DH, Semple MN. Transformation of temporal properties between auditory midbrain and cortex in the awake Mongolian gerbil. *J Neurosci* 27: 6091–6102, 2007.

Winter IM, Palmer AR. Responses of single units in the anteroventral cochlear nucleus of the guinea pig. *Hear Res* 44: 161–178, 1990.

Yin TC, Chan JC. Interaural time sensitivity in medial superior olive of cat. *J Neurophysiol* 64: 465–488, 1990.

Yin TC, Kuwada S. Binaural interaction in low-frequency neurons in inferior colliculus of the cat. III. Effects of changing frequency. *J Neurophysiol* 50: 1020–1042, 1983.